

# SPATIAL AND TEMPORAL DISTRIBUTIONS OF IONOSPHERIC CURRENTS-2. LONGITUDE-LOCAL TIME CROSS SECTIONS OF EQUATORIAL ELECTROJET CURRENT DENSITY, INTENSITY AND TOTAL FORWARD CURRENT

C. AGODI ONWUMECHILI, S. O . OKO. and P. O. EZEMA

(Received 12 January 2001 ; Revision accepted 9 May, 2001)

## ABSTRACT

A comprehensive analysis of Polar Orbiting Geomagnetic Observatory (POGO) satellites data for 1967 –1969 produced 894 values of each equatorial electrojet (EEJ) parameter. For each parameter the values are organized into a table of 36 longitude rows for 0°, 10°, 20°, 30°, ..... 350°E and 7 local time hour columns for 09, 10, 11, ..... 15 hour. It thus becomes possible to produce longitude-local time cross section for each parameter. The daytime means of the 7 parameters necessary for the construction of the longitude-local time cross sections of equatorial electrojet current density, intensity and total forward current are given for the 36 selected longitudes. The first longitude-local time cross sections of EEJ current density, intensity and total forward current are presented. They display the following features: (a) along any longitude the EEJ current retains a diurnal maximum at noontime; (b) at any local time the EEJ current has maxima at 100°E, 190°E and 290°E, and minima at about 20°E, 60°E, 140°E and 230E; and (c) three contour cells of high current strength manifest with their peaks on the average at (12 h, 100°E), (11 h, 190E) and (12 h, 290°E). On the whole, the longitude-local time cross sections of EEJ current density, intensity and total forward current are complex.

**Key words:** longitude-local time cross sections, current intensity, total forward current.

## 1. INTRODUCTION

The continuous distribution of current density model of Onwumechili (1965) is employed in this paper. In this model the eastward current density  $j(r, \varnothing)$  at the point  $(r, \varnothing)$  is

$$j = j_0 \frac{a^2(a^2 + \alpha\phi^2)}{(a^2 + \phi^2)^2} \frac{b^2(b^2 + \beta r^2)}{(b^2 + r^2)^2} \quad (1)$$

where  $\varnothing$  is southward latitude,  $r$  is radial distance,  $j_0$  is the peak current density at the current centre where  $\varnothing = 0 = r$  and longitude ( $\lambda$ ) is eastwards. The  $a$  and  $b$  are scale latitude and scale radial distance respectively, and  $\alpha$  and  $\beta$  are dimensionless constants controlling the distribution of current latitudinally and radially respectively.

The current intensity  $J$  is obtained by integrating the current density vertically with respect to  $r$  through its altitude extent from  $-L_2$  to  $L_2$ . Thus

$$J = J_0 \frac{a^2(a^2 + \alpha\phi^2)}{(a^2 + \phi^2)^2}, \text{ and} \quad (2)$$

$$J_0 = bj_0 \left[ \frac{(1 - \beta)bL_2}{(b^2 + L_2^2)} + (1 + \beta) \tan^{-1} \frac{b}{L_2} \right], \quad (3)$$

where  $J_0$  is the peak current intensity at the current centre. The total forward current  $I_F$  is obtained by integrating Eq. (2) latitudinally with respect to  $\phi$  from the northern focus  $-w$  to the southern focus  $w$ . Because

$$w^2 = -a^2/\alpha \quad (4)$$

this is more conveniently expressed as

$$I_F = aJ_0 [ (-\alpha)^{1/2} + (1 + \alpha) \tan^{-1} \frac{1}{(-\alpha)^{1/2}} ] \quad (5)$$

All the parameters are implicit functions of longitude and local time because the model is applied separately to each longitude and each local time. Thus the current density  $j$  Eq. (1) is a function of altitude, latitude, longitude and local time. Therefore, the current density has six cross sections, namely: altitude-latitude, altitude-longitude, altitude-local time, latitude-longitude, latitude-local time and longitude-local time cross sections. The current intensity  $J$  of Eq. (2) is a function of latitude, longitude and local time. Therefore the current intensity has three cross sections, namely: latitude-longitude, latitude-local time and longitude-local time cross sections. Accordingly, the total forward current  $I_F$  of Eq. (5) is a function of longitude and local time. It has only one cross section, namely, longitude-local time cross section. There are therefore, 10 cross sections of current in all: six of  $j$ , three of  $J$  and one of  $I_F$ . The objective of the group of papers among which is the present paper is to present all the ten possible cross sections of the equatorial electrojet (EEJ) plus its subsolar elevation.

For now only the first of the 10 cross sections has been published before in some form as discussed in paper 1. Although Onwumechili spoke on some of the other 9 cross sections at the IUGG General Assembly at Vienna, August 1991, they are yet to be published in a journal. Singh and Cole (1987), Untiedt (1967), Sugiura and Poros (1969), and Davis et al (1967) worked on altitude-latitude cross sections however, no work has been done on longitude-local time cross section. For now, we are not aware that anybody else has published anything on any of the nine cross sections. This Paper 2 discusses the longitude-local time cross sections of EEJ current density, intensity and total forward current.

## 2 THEORETICAL CALCULATIONS AND ANALYSIS

The geomagnetic components are normally given as X northwards, Y eastwards and Z vertically downwards. It is convenient to adopt a corresponding coordinate system. Accordingly, we measure latitude as  $x$  northwards,  $y$  as longitude eastwards and radial distance as  $z$  downwards from the current centre. Thus in the above equations  $x$  replaces  $\phi$  and  $z$  replaces  $r$

On inserting Eq. (1), in the convenient coordinate system, into the expression for Biot-Savart law and integrating vertically and latitudinally through the vertical and latitudinal extents of the current we get

$$\begin{aligned} (sg. z) P^4 X &= \frac{1}{2} k [(1 + \beta) (v + \alpha v + 2a) (v + a)^2 \\ &+ (v + \alpha v + 2\alpha a) (u + \beta u + 3b - \beta b) (u + b) \\ &+ 8(1 - \alpha) (1 - \beta) ab (u + b)] \end{aligned} \quad (6)$$

$$\begin{aligned} (sg. x) P^4 Z &= \frac{1}{2} k [(1 + \alpha) (u + \beta u + 2b) (u + b)^2 \\ &+ (u + \beta u + 2\beta b) (v + \alpha v + 3a - \alpha a) (v + a)] \end{aligned} \quad (7)$$

$$\text{where } P^2 = (u + b)^2 + (v + a)^2 \quad (8)$$

$$k = 0.1 \pi^2 abj_0 \quad (9)$$

$$k(1 + \beta) = 0.2\pi aJ_0 \quad (10)$$

$$u = |x| \text{ and } v = |z|,$$

sg.  $x = x/u$ , and sg.  $z = z/v$

Thus the expressions for  $X$  and  $Z$  each contains the desired parameters of the model:  $j_0$ ,  $a$ ,  $\alpha$ ,  $b$ , and  $\beta$ . Onwumechili and Ezema (1992) have described how the Polar Orbiting Geomagnetic Observatory (POGO) satellites magnetic measurements are fitted with the model to obtain the five parameters at 36 selected longitudes:  $0^\circ$ ,  $10^\circ$ ,  $20^\circ$ ,  $30^\circ$ , ....  $350^\circ$ E. The data are available for only 09, 10, 11, 12, 13, 14 and 15 hours local time. With these, the peak forward current intensity  $J_0$  is calculated from Eq. (10) and the total forward current  $I_F$  is calculated from Eq. (5). In these calculations, it is important to use the  $j_0$ ,  $a$ ,  $\alpha$ ,  $b$  and  $\beta$  appropriate for the local time and longitude of the parameter being calculated.

Table 1 Average values from 09 hour to 15hr local time of certain parameters for equatorial electrojet current at intervals of  $10^\circ$  longitude derived from POGO satellites data.

Longitude Degree E	$j_0$ A/km <sup>2</sup>	$a$ Degree	$\alpha$	$b$ km	$\beta$	$J_0$ A/km	$I_F$ Amperes
0	6.00	3.3932	-1.5122	8.9583	0.5242	128	41905
10	4.90	3.4131	-1.5148	9.0082	0.5233	103	33777
20	4.58	3.4268	-1.5113	9.0701	0.5361	97	31738
30	4.95	3.3934	-1.5158	9.1005	0.5324	107	35518
40	5.13	3.4151	-1.5288	9.1194	0.5234	111	37306
50	4.86	3.4883	-1.5339	9.2083	0.5196	106	36395
60	5.05	3.3181	-1.5085	8.8816	0.5102	100	31509
70	6.92	3.2599	-1.5160	8.6599	0.5141	137	43218
80	9.53	3.1933	-1.5083	8.3766	0.5139	191	61443
90	10.96	3.4368	-1.5389	8.8660	0.5310	233	78053
100	11.44	3.5207	-1.5365	9.0927	0.5438	252	84397
110	9.75	3.5027	-1.5353	9.0290	0.5484	212	71891
120	7.88	3.6097	-1.5254	8.9636	0.5525	170	57712
130	5.13	3.4375	-1.5216	8.9594	0.5480	109	35770
140	4.80	3.4498	-1.5206	9.0361	0.5437	105	35405
150	4.89	3.4742	-1.5636	9.0001	0.5283	104	35190
160	6.43	3.4153	-1.5601	8.8761	0.5197	132	43390
170	8.18	3.3534	-1.5450	8.7664	0.5164	167	53832
180	10.04	3.2935	-1.5217	8.7369	0.5210	208	65852
190	10.58	3.2988	-1.5301	8.7638	0.5202	222	71548
200	9.02	3.4143	-1.5583	8.8767	0.5231	191	62512
210	7.21	3.4141	-1.5452	8.9482	0.5251	153	50575
220	5.94	3.4243	-1.5337	8.9522	0.5302	126	41555
230	5.95	3.3540	-1.5285	8.8096	0.5231	123	38357
240	6.39	3.4066	-1.5132	8.8881	0.5252	134	42774
250	7.47	3.5081	-1.5328	9.0430	0.5229	161	53441
260	8.48	3.4777	-1.5437	9.0381	0.5260	181	59932
270	10.11	3.4729	-1.55812	9.1241	0.5350	219	73208
280	11.20	3.3792	-1.5571	9.0146	0.5425	142	79684
290	12.42	3.4871	-1.5362	9.0435	0.5439	269	90916
300	11.71	3.5359	-1.5142	9.1473	0.5336	250	84848
310	10.10	3.5148	-1.5390	9.0614	0.5177	214	71784
320	7.80	3.3866	-1.5582	9.0906	0.5047	168	55763
330	6.21	3.3671	-1.5552	9.0708	0.5077	136	44796
340	5.98	3.3961	-1.5407	9.1496	0.5218	134	44177
350	6.04	3.3564	-1.5099	8.9547	0.5203	131	42080
Mean	7.61	3.4164	-1.5332	8.9635	0.5270	162	53396
S.D	2.40	0.0830	0.0183	0.1625	0.0119	52	17489

The authors analyzed 894 profiles of POGO magnetic data for 1967 – 1969. Each profile yields one value of each parameter. The 894 values of each parameter are organized into a matrix table of 36 rows for longitude  $\lambda = 0^\circ, 10^\circ, 20^\circ, \dots, 350^\circ$ E and 7 columns for local time hours  $t = 09, 10, 11, \dots, 15$  hour. Instead of 7 such tables for  $j_0$ ,  $a$ ,  $\alpha$ ,  $b$ ,  $\beta$ ,  $J_0$  and  $I_F$  respectively, we give only their daytime means at each of the 36 selected longitudes in Table 1.

### 3 LONGITUDE-LOCAL TIME CROSS SECTION OF EQUATORIAL ELECTROJET CURRENT DENSITY

The matrix table of values of  $j_0$  Akm<sup>-2</sup> consisting of 36 longitude rows for  $\lambda = 0^\circ, 10^\circ, 20^\circ, \dots, 350^\circ$ E and 7 local time hour columns for  $t = 09, 10, 11, \dots, 15$  hours is used for constructing the longitude-local time cross section. The matrix elements are plotted. By interpolation, the contours of 18, 16, 14, 12, 10, 8, 6, 4, and 2 Akm<sup>-2</sup> in Fig. 1 are plotted.

Although Fig. 1 looks complex the following considerations assist in its understanding. The daytime mean  $j_0$  in Table 1 has maxima around  $100^\circ\text{E}$ ,  $190^\circ\text{E}$  and  $290^\circ\text{E}$ , and minima around  $20^\circ\text{E}$ ,  $140^\circ\text{E}$  and  $220^\circ\text{E}$ . This is a reflection of the structure at most of the local time hours. Thus for any selected local time in Fig. 1 the variation of  $j_0$  with longitude is as suggested by the daytime mean  $j_0$  in Table 1.

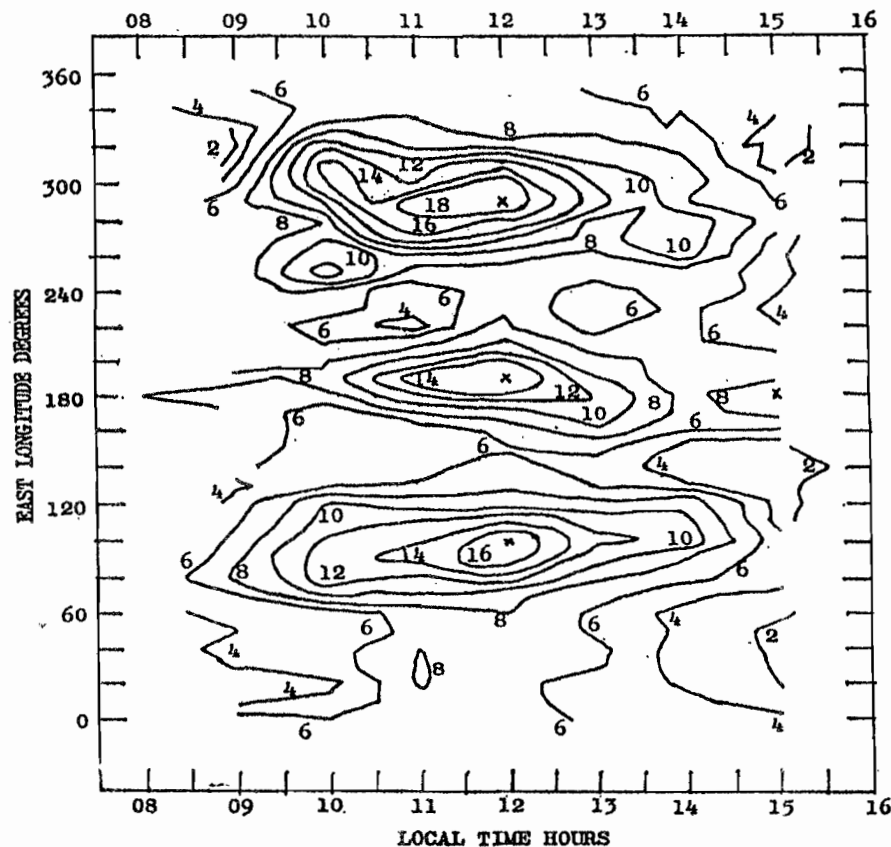


Fig. 1 Longitude-local time cross section of the equatorial electrojet peak current density  $j_0$   $\text{A km}^{-2}$ , showing contours of 18, 16, 14, 12, 10, 8, 6, 4, and 2  $\text{A km}^{-2}$ . Peaks of the major contour cells occur at (12h,  $100^\circ\text{E}$ ), (12h,  $190^\circ\text{E}$ ) and (12h,  $290^\circ\text{E}$ ). Contours outside 09 hr to 15 hr are extrapolations.

It is well-known, as is also suggested by Table 1 of paper 1, that the EEJ becomes more intense towards local noon, and indeed attains a maximum strength around local noon. Accordingly, for any selected longitude in Fig. 1, the EEJ peak current density  $j_0$  increases from 09 hr to a maximum around local noon and then decreases towards evening. Indeed, in this case the diurnal peak occurred at local noon at most latitudes.

With the above variations of  $j_0$  with longitude and local time it is then easy to understand how contour cells of high current density are centred at local noon at the three longitudes where the current density is a maximum. The dominating features of Fig. 1 are clearly: the contour cells peaking at (12h,  $100^\circ\text{E}$ ), (12h,  $190^\circ\text{E}$ ) and (12h,  $290^\circ\text{E}$ ), and the troughs at  $140^\circ\text{E}$  and  $220^\circ\text{E}$ .

The cross section in Fig. 1 corresponds to a position at the current centre. Consider any fixed values  $r_1$  and  $\varnothing_1$ . It is clear from Eq. (1) that for any point other than the current centre, such as  $(r_1, \varnothing_1)$ ,  $(0, \varnothing_1)$  or  $(r_1, 0)$ , the longitude-local time cross section of the current density  $j$  has the same pattern as Fig. 1 but the current density at every point  $(t, \lambda)$  in the cross section is smaller than at the corresponding point in Fig. 1

## 4 LONGITUDE-LOCAL TIME CROSS SECTION OF EQUATORIAL ELECTROJET CURRENT INTENSITY

The longitude-local time cross section of equatorial electrojet (EEJ) peak current intensity  $J_0$  is constructed from the values of  $J_0$  obtained as described in section 2 above. The 894

values of  $J_0$  are organized into a matrix table of 36 longitude rows for  $\lambda = 0^\circ, 10^\circ, 20^\circ, 30^\circ, \dots, 350^\circ\text{E}$  and 7 columns of local time hours for  $t = 09, 10, 11, \dots, 15$  hours. The matrix elements are plotted. By interpolation the contours of 400, 300, 250, 200, 150, 100 and 50  $\text{Akm}^{-1}$  in Fig. 2 are calculated and plotted.

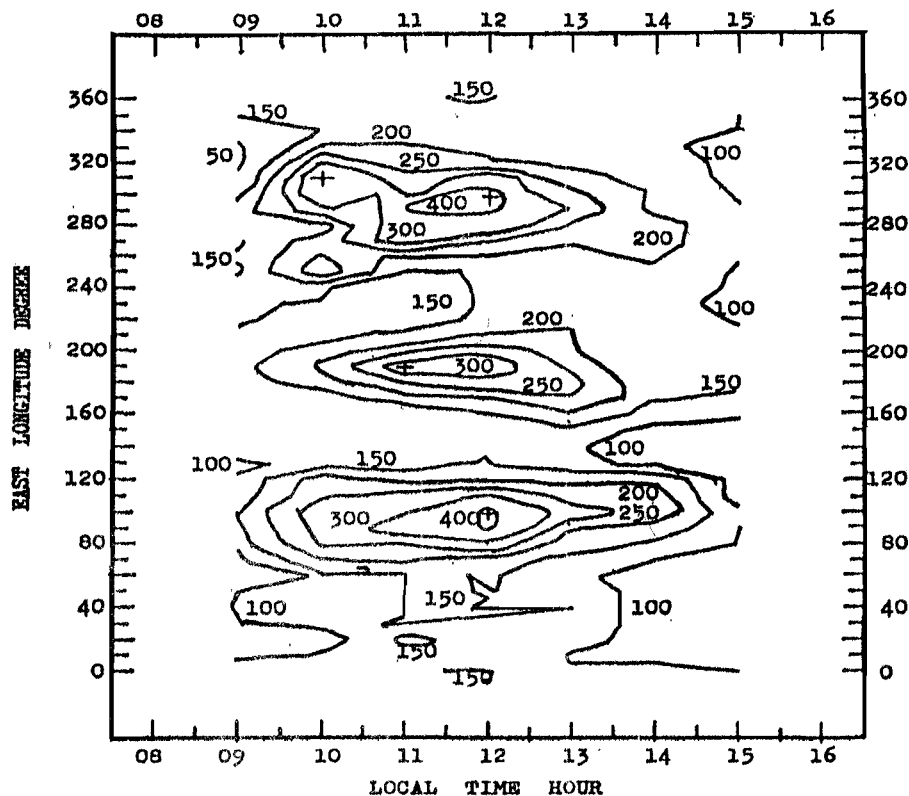


Fig. 2 Longitude-local time cross section of the equatorial electrojet peak current intensity  $J_0 \text{ Akm}^{-1}$ , showing contours of 400, 300, 250, 200, 150, 100 and 50  $\text{Akm}^{-1}$ . Peaks of the major contour cells occur at (12h,  $100^\circ\text{E}$ ), (11h,  $190^\circ\text{E}$ ) and (12h,  $290^\circ\text{E}$ ).

In general, Fig. 2 resembles Fig. 1. The daytime mean  $J_0$  in Table 1 has maxima at  $100^\circ\text{E}$ ,  $190^\circ\text{E}$  and  $290^\circ\text{E}$  and minima around  $20^\circ\text{E}$ ,  $150^\circ\text{E}$ , and  $230^\circ\text{E}$ . There are however notable exceptions like 10 hr when the last maximum occurred at  $310^\circ\text{E}$  instead of at  $290^\circ\text{E}$ ; and 14 hr when the first minimum occurred at  $40^\circ\text{E}$  instead of  $20^\circ\text{E}$ .

As expected in section C, Fig. 2 shows that for a selected longitude,  $J_0$  increases from morning to a maximum around local noon and then decreases towards evening. Again there are notable exceptions. Apart from the above when the diurnal maximum for  $310^\circ\text{E}$  occurs at 10 hr; the maximum for  $290^\circ\text{E}$  occurs at 11 hr, and the maximum for  $260^\circ\text{E}$  occurs at 14hr local time.

Again the commanding features of Fig. 2 are the three contour cells of high current intensity and the intervening troughs at about  $140^\circ\text{E}$  and  $230^\circ\text{E}$ . The contour cells of high current intensity in this case peak at (12h,  $100^\circ\text{E}$ ), (11h,  $190^\circ\text{E}$ ) and (12h,  $290^\circ\text{E}$ ).

The longitude local time cross section of  $J_0$  in Fig. 2 corresponds to the point at the centre of the current where  $\varnothing = 0$ . It is clear from Eq. (2) that for any other point where  $\varnothing = \varnothing_1$ , the longitude-local time cross section for the current intensity  $J$ , has the same pattern as Fig. 2 but the current intensity at every point  $(t, \lambda)$  in the cross section is smaller than at the corresponding point in Fig. 2.

## 5 LONGITUDE-LOCAL TIME CROSS SECTION OF EQUATORIAL ELECTROJET TOTAL FORWARD CURRENT

The matrix table of values of total forward current  $I_f \text{ kA}$  with 36 longitude rows for  $\lambda = 0^\circ, 10^\circ, 20^\circ, 30^\circ, \dots, 350^\circ\text{E}$  and 7 local time hour columns for  $t = 09, 10, 11, \dots, 15$  hour is calculated from Eq. (5) as described in section b. The values are plotted. Interpolations are then calculated and plotted to produce the longitude-local time contours of 120, 100, 80, 60, 40, and 20 kA shown in Fig. 3

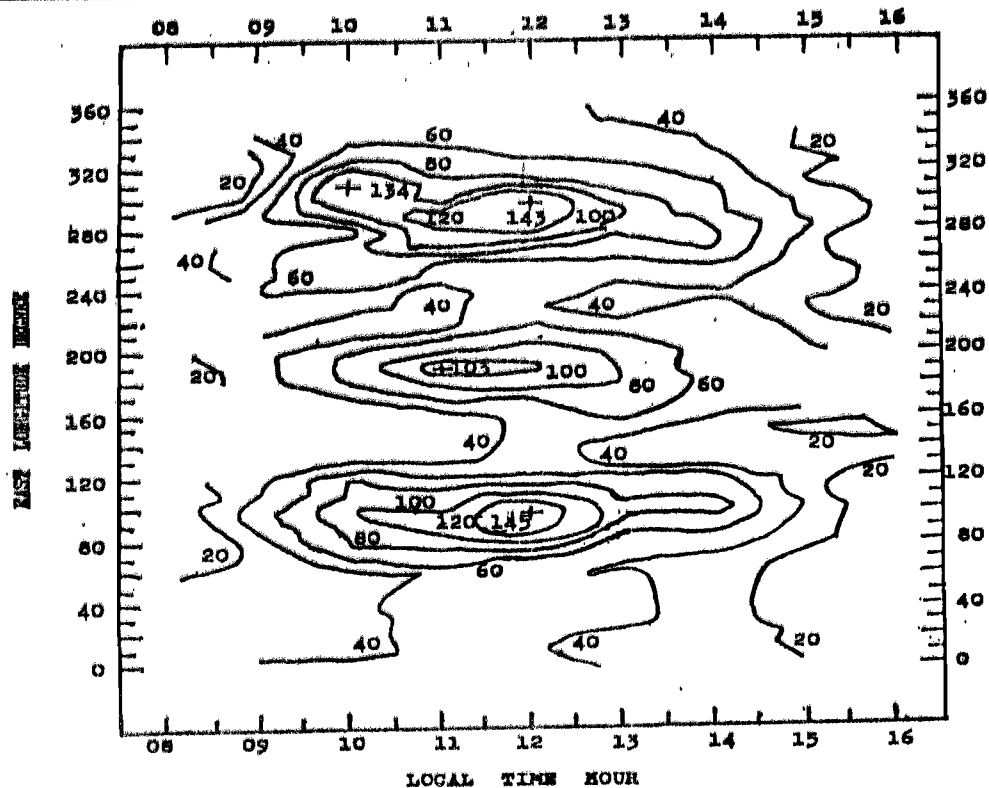


Fig. 3 Longitude-local time cross sections of the equatorial electrojet total forward current  $I_f$  kA, showing contours of 120, 100, 80, 60, 40 and 20 kA. Peaks of the major contour cells occur at (12 h, 100°E), (11 h, 190°E) and (12 h, 300°E). Contours outside 09 hr to 15 hr are extrapolations.

In general, Fig. 3 resembles the corresponding longitude-local time cross sections of current density in Fig. 1 and of current intensity in Fig. 2. Table 1 shows that the daytime mean  $I_f$  has maxima at 100°E, 190°E and 290°E; and minima at 20°E, 60°E, 150°E, and 230°E. Similarly, at most local times the  $I_f$  has maxima and minima close to the above longitudes. However, all the exceptions mentioned in the case of peak current intensity  $J_0$  also occur in the case of  $I_f$ . In addition, the last maximum at 14 hr occurs at 270°E.

Generally, in keeping with the discussions of  $j_0$  and  $J_0$ , at a given longitude, the total forward current  $I_f$  rises to the diurnal maximum around noontime and then declines. However, there are several exceptions, the most notable being the diurnal maximum at 10 hr along 120°E, 250°E, 260°E and 310°E.

The three contour cells of high total current and their associated troughs are even more outstanding in Fig. 3 than in Fig. 1 and Fig. 2. In Fig. 3 the peaks of the cells are located at (12 h, 100°E), (11h, 190°E) and (12h, 300°E). The two most conspicuous troughs occur at 140°E and 230°E.

## 6

## CONCLUSIONS

A comprehensive analysis of the POGO satellites data of 1967–1968 has been performed with Onwumechili's continuous distribution of current density model. This yielded 894 values of each parameter of the model and each physical parameter of the equatorial electrojet (EEJ). For each parameter the 894 values are organized into a matrix table of 36 longitude rows for  $\lambda = 0^\circ, 10^\circ, 20^\circ, 30^\circ, \dots, 350^\circ$ E and 7 local time hour columns for  $t = 09, 10, 11, \dots, 15$  hour. It is thus possible to produce the longitude-local time cross section for each parameter.

The longitude-local time cross sections of EEJ current density, intensity and total current are similar but complex. It shows that along a given meridian of longitude the EEJ current strength exhibits a diurnal maximum near local noon. And at a given time in daytime, EEJ current strength has maxima at about 100°E, 190°E, and 290°E and has minima at about 20°E, 60°E, 140°E and 230°E. However, both the variations with local time and longitude manifest minor variations